See related Commentary on page 1513

The American Journal of Pathology, Vol. 181, No. 5, November 2012
Copyright © 2012 American Society for Investigative Pathology.
Published by Elsevier Inc. All rights reserved.
http://dx.doi.org/10.1016/j.ajpath.2012.07.024

Animal Models

Chronic Intermittent Hypoxia Exposure Induces Atherosclerosis in ApoE Knockout Mice

Role of NF-κB p50

Guoqiang Fang, Dongmei Song, Xiaobing Ye, Sun-zhong Mao, Gang Liu, and Shu Fang Liu

From the Centers for Heart and Lung Research, and Pulmonary and Sleep Medicine, the Feinstein Institute for Medical Research, Manhasset, New York

Current animal models of chronic intermittent hypoxia (CIH)-induced atherosclerosis have limitations. Mechanisms of CIH-induced atherosclerosis are poorly understood. This study tested new mouse models of CIH-induced atherosclerosis and defined the role of NF-κB p50 in CIH-induced atherosclerosis. Mice deficient in apolipoprotein E (ApoE-KO) or in both *ApoE* and *p50* genes (ApoE-p50-DKO) were exposed to sham or CIH. Atherosclerotic lesions on aortic preparations were analyzed. CIH exposure caused atherosclerosis in ApoE-KO mice fed a normal chow diet and with no preexisting atherosclerotic condition in an exposure time-dependent manner. CIH caused more pronounced atherosclerotic lesions in ApoE-p50-DKO mice on a normal chow diet without preexisting atherosclerosis. ApoE-KO and ApoE-p50-DKO mice exposed to CIH for 30 and 9 weeks, respectively, displayed similar areas of atherosclerotic lesions on cross sections of aortic root. P50 gene deletion in ApoE-p50-DKO mice significantly augmented CIH-induced serum levels of tumor necrosis factor-α and IL-6, aortic tumor necrosis factor-α, and inducible nitric oxide synthase expression and aortic infiltration of Mac3-positive macrophages. CIH caused a greater elevation in serum cholesterol level in ApoE-p50-DKO than in ApoE-KO mice. CIH downregulated hepatic low-density lipoprotein receptor and HMG-CoA reductase expression in ApoE-p50-DKO but not in ApoE-KO mice. We found two new mouse models that are useful for studying mechanisms and pathways of CIH-induced atherosclerosis. We showed that NF-κB p50 protects against CIH-induced atherosclerosis by inhibiting vascular inflammation and hypercholesterolemia. ***(Am J Pathol 2012, 181: 1530–1539; http://dx.doi.org/10.1016/j.ajpath.2012.07.024)***

Patients with obstructive sleep apnea (OSA) have increased prevalence of coronary and cerebral vascular diseases and stroke,[1–7] common consequences of atherosclerosis. The molecular mechanisms linking OSA to atherosclerosis remain largely unknown. Because chronic intermittent hypoxia (CIH) is a prominent feature of OSA,[8,9] there has been a great interest in developing animal model of CIH-induced atherosclerosis and in understanding how CIH exposure causes atherosclerosis.[10–14]

In wild-type mice, CIH exposure causes hypertension,[15,16] dyslipidemia,[10,11,17,18] vascular inflammation,[19,20] and vascular remodeling,[20] but it does not cause atherosclerosis,[10] even after long-term (8.3 months) exposure.[21] To overcome this problem, Savransky et al[10] found that a combined exposure to CIH and a high-cholesterol diet (HCD) causes atherosclerosis in wild-type mice. Subsequently, several studies have used the "CIH+HCD" model to investigate mechanisms of CIH-induced atherosclerosis in wild-type mice and in mice deficient in apolipoprotein E gene (ApoE-KO).[10–13] Although useful and valuable, this model has limitations.[10–13] HCD per se is a strong inducer of atherosclerosis. In fact, ApoE-KO mice fed a HCD is the most widely used model of experimental atherosclerosis.[22,23] In the presence of this confounding factor, it would be extremely difficult to assess the independent causative effect of CIH on atherogenesis and on plague pathology. Recognizing this limitation, Arnaud et al[14] fed 15- or 20-week-old ApoE-KO mice that have developed intermediate or fibrous atherosclerotic lesions a normal chow

Supported by a grant from the American Heart Association (0655794T).

Accepted for publication July 18, 2012.

G.F. and D.S. contributed equally to this work.

Address reprint requests to Shu Fang Liu, M.D., Ph.D., The Feinstein Institute for Medical Research, 350 Community Dr, Manhasset, NY 11030. E-mail: Sliu@lij.edu.

diet (ND) and exposed them to CIH and found that 2 weeks of CIH exposure exacerbated preexisting atherosclerosis. This model is useful for evaluating the effect of CIH on the progression of atherosclerosis, but it is not useful for studying how CIH initiates atherogenesis and how CIH causes atherosclerotic lesions. To uncover an independent causal role of CIH in atherosclerosis, it is ideal to expose animals with no preexisting atherosclerotic pathology to CIH in the absence of other potential atherogenic factors. Such a model of CIH-induced atherosclerosis has not been described.

Although CIH has been found to facilitate the development and progression of atherosclerosis, the mechanisms mediating the CIH effect remain incompletely understood. CIH activates NF-κB and induces the expression of NF-κB-dependent genes.[19,20] Patients with OSA have an increased NF-κB activity in circulating neutrophils and monocytes[24] and elevated serum levels of NF-κB-dependent gene products.[24–27] NF-κB-mediated inflammatory pathways play integrated roles in the classic HCD-induced atherosclerosis.[28,29] Activation of the NF-κB pathway may be a major mechanism of CIH-induced atherosclerosis. The mechanistic role of NF-κB in CIH-evoked atherogenic response has not been studied.

The aims of this study are twofold: to develop new mouse models of CIH-induced atherosclerosis and to define the role of NF-κB pathway in CIH-induced atherosclerosis. ApoE-KO mice with no preexisting atherosclerotic lesions were fed a ND and exposed to CIH. This model avoids the confounding by HCD and allows studying CIH-induced early molecular and cellular events that lead to atherosclerosis. We blocked NF-κB activation in mice deficient in *ApoE* and *NF-κB p50* gene (ApoE-p50-DKO). We chose to use p50-KO mice, because this mouse strain can tolerate the harsh experimental condition of long-term CIH exposure, compared with other NF-κB mutant mouse strains. We found that CIH exposure per se causes atherosclerosis and that NF-κB p50 plays a protective role in CIH-induced atherosclerosis.

Materials and Methods

CIH Exposure Protocol

ApoE-KO and mice deficient in NF-κB p50 gene (p50-KO) were purchased from The Jackson Laboratory (Bar Harbor, ME). ApoE-p50-DKO mice were created by crossbreeding between ApoE-KO and p50-KO mice (all on C57BL/J genetic background). To avoid potential gender effect, an equal number of male and female mice were included in each study group. Study protocols were approved by the institutional animal care and use committee of the Feinstein Institute for Medical Research. Mice were fed a ND and exposed to sham or CIH, starting at 7 weeks of age. Mice in the HCD-positive control group were fed a HCD. To mimic the cyclic episodes of hypoxia and its subsequent re-oxygenation seen in patients with OSA, we placed sham- and CIH-exposed mice in separate, but identical Plexiglas exposure chambers that we have previously described in detail.[19] Fractional oxygen concentration in the exposure chamber was reduced to a nadir of 6.0% to 6.5%, stabilized at that level for 5 to 7 seconds, and then gradually increased to 21% over the next 30 seconds by infusion of nitrogen or air into the chambers by computer-controlled solenoid valves. This cycle was repeated every minute over 8 hours during the animals' diurnal sleep period for days as designed. Sham-exposed mice were exposed to similar handling but room air was used instead of nitrogen.

To characterize the oxygen profile of our CIH protocol, 5 mice were exposed to CIH for 5 days and anesthetized with tribromoenthanol, and the carotid artery was cannulated. Arterial blood was collected when fractional oxygen concentration in the chamber was at 21% and 6% to 6.5%, respectively, and blood gases were analyzed. Another cohort of 5 mice was exposed to CIH for 5 days, and pulse oximeter oxygen saturation was measured with mouse pulse oximetry at day 6.

Tissue Harvest and Atherosclerotic Lesion Analysis

At conclusion of exposure protocols, mice were deprived of food for 8 hours and sacrificed, and blood, heart, and aorta were collected. For *en face* analysis of atherosclerotic lesions on aorta, the aortic tree was perfused with PBS, opened longitudinally starting from approximately 5 mm distal to the aortic root to the iliac bifurcation, fixed in a mixture of 5% sucrose and 10% buffered formalin, and stained with Sudan IV solution.[30,31]

For analysis of atherosclerotic lesions on cross section of the aortic root, the heart was embedded in OCT medium, and serial 6-μm cryostat heart/aortic sections centered on the aortic valves were prepared. These sections were stained with oil red O and hematoxylin as previously described.[30,31] Images of cross sections and *en face* aortic preparations were captured with a Nikon DS camera (Nikon, Melville, NY). The whole atherosclerotic lesion areas were quantified in a blind fashion with the use of Nikon NIS-Elements Research Software version 3.0 and expressed as a percentage of the total aortic area or as $\times 10^4$ μm (cross section).

Electrophoretic Mobility Shift Assay

Nuclear and cytoplasmic proteins were extracted from aorta and liver, and NF-κB binding activity was measured by electrophoretic mobility shift assay with the use of ^{32}P-labeled NF-κB consensus oligonucleotide as we have previously described.[32] Each individual member of the NF-κB family was identified by supershift assay with the use of antibody (1 μg) against p50, p52, p65, Rel B, and C-Rel protein (Santa Cruz Biotechnology, Santa Cruz, CA).

RT-qPCR

Total RNA was extracted with Trizol reagent (Invitrogen, Carlsbad, CA) and treated with DNase I to remove traces of genomic DNA. RNA sample was subjected to quanti-

tative RT-PCR (RT-qPCR) with the use of TaqMan One-Step RT-PCR Master Mix Reagents (Applied Biosystems, Foster City, CA), and gene-specific primers and probes. The gene-specific probes were 78 for HMG-CoA reductase (HMGCR), 64 for low-density lipoprotein (LDL) receptor, 1 for ATP-binding cassette transporter A1 (ABCA1), 2 for scavenger receptor class B1 (SR-B1), and 74 for sterol regulatory element-binding factor (SREBF)-2 (Roche Universal Probe Library, Mannheim, Germany). Primers used were HMGCR: forward, 5′-TGATTGGAGTTGGCACCAT-3′, and reverse, 5′-TGGCCAACACTGACATGC-3′; LDL receptor: forward, 5′-GATGGCTATACCTACCCCTCAA-3′, and reverse, 5′-TGCTCATGCCACATCGTC-3′; ABCA1: forward, 5′-GCAGATCAAGCATCCCAACT-3′, and reverse, 5′-CCAGAGAATGTTTCATTGTCCA-3′; SR-B1: forward, 5′-GCCCATCATCTGCCAACT-3′, and reverse, 5′-TCCTGGGAGCCCTTTTTACT-3′; and SREBF-2: forward, 5′-ACCTAGACCTCGCCAAAGGT-3′, and reverse, 5′-GCACGGATAAGCAGGTTTGT-3′. RT-qPCR was performed in 7900 HT thermocycler (Applied Biosystems, Foster City, CA). Results were analyzed with the $\Delta\Delta C_t$ method. Expression of specific genes was normalized to β-actin gene (TaqMan RNA Reagents; Applied Biosystems).

Western Blot Analysis

Equal amounts of proteins were separated on 7.5% to 10% SDS-PAGE slab gel under denaturing conditions. Tissue levels of tumor necrosis factor (TNF) receptor-associated factor 3 (TRAF3), p100, I-κBα, and actin were detected by Western blot analysis, as we have previously described.[32]

Measurement of Serum Levels of Lipids, Lipoproteins, and Cytokines

Serum levels of total cholesterol and triglycerides were measured with cholesterol and triglyceride reagent sets (Pointe Scientific, Canton, MI). Serum levels of high-density lipoprotein (HDL) and LDL/very LDL cholesterol were measured with EnzyChrom HDL and LDL/very LDL assay kit (BioAssay Systems, Hayward, CA). Serum levels of TNF-α and IL-6 were measured with TNF-α and IL-6 enzyme-linked immunosorbent assay kits (ELISA) (eBiosciences, San Diego, CA).

Immunohistochemical Staining

Cryosections (6 μm) were prepared, fixed, permeabilized, blocked in blocking solution, and incubated with anti-inducible nitric oxide synthase (iNOS), anti-TNF-α, or anti-Mac3 antibodies (Santa Cruz Biotechnology) as we have previously described.[33] Specific binding was detected with biotinylated secondary antibody–horseradish peroxidase complexes with the use of VECTASTAIN Elite ABC kits (Vector Laboratories, Burlingame, CA). Antigen-antibody complexes were visualized with 3′, 3′-diamino benzidine (Vector Laboratories). Sections were counterstained with hematoxylin, mounted, and viewed under light microscope. Total and iNOS (or TNF-α) positive areas were quantified in five random microscopic fields per aortic section under the same magnification. The accumulated iNOS (or TNF-α) positive area from the five microscopic fields was expressed as a percentage of the accumulated total analyzed area of aortic wall.

Statistical Analysis

Data were expressed as means ± SEMs and were analyzed with unpaired *t* test or Mann-Whitney rank test for comparing two groups and analysis of variance or Kruskal-Wallis rank test for comparing multiple groups, followed by Holm-Sidak method or Student-Newman-Keuls method for *post hoc* analysis. The null hypothesis was rejected at the 5% level.

Results

Body Weight and Oxygen Profiles

Body weight was comparable between the respective sham and CIH groups at the commencement of exposure protocols. After 9 weeks of CIH exposure, body weight for the ApoE-KO-sham, ApoE-KO-CIH, ApoE-p50-DKO-sham, and ApoE-p50-DKO-CIH groups were 24.2 ± 1.2, 22.9 ± 0.7, 23.9 ± 1.0, and 23.1 ± 0.9 g, respectively. After 30 weeks of exposure, mean body weights for the sham and CIH groups of ApoE-KO mice were 26.8 ± 1.3 and 25.3 ± 1.4 g, respectively.

Blood gas analysis on a group of anesthetized mice and mouse pulse oximetry measurement on another cohort of awake mice showed that a decline in fractional oxygen concentration from 20.9% to a nadir of 6% over the 30-second hypoxic period resulted in a drop in partial pressure of arterial oxygen from 95.3 ± 5.6 to 45 ± 1.5 mmHg, and a drop in pulse oximeter oxygen saturation from 97.3% ± 0.3% to 79.6% ± 1.4%. Our results are consistent with a report showing that partial pressure of arterial oxygen dropped from 88 ± 3 mmHg at room air to 47 ± 2 mmHg at the nadir of 6% O_2 in conscious and chronically cannulated mice.[34] Thus, our mouse model produced a level of hypoxia that resembled moderate-to-severe OSA and a rate of hypoxia (60 events/hour) which simulates severe OSA.[8,9]

CIH Exposure Causes Atherosclerosis in ApoE-KO Mice in an Exposure Time-Dependent Manner

Two cohorts of ApoE-KO mice were fed a ND and were exposed to sham or CIH for 9 and 30 weeks, respectively. No atherosclerotic lesions were detectable on both aortic preparations from ApoE-KO mice at the beginning of CIH exposure (Figure 1, A and B). As expected, older ApoE-KO mice developed atherosclerosis spontaneously. After 9 weeks of CIH exposure, atherosclerotic lesion areas on *en face* aortic preparations were similar between sham- and CIH-exposed mice, but on cross sections of aortic root the atherosclerotic lesion areas

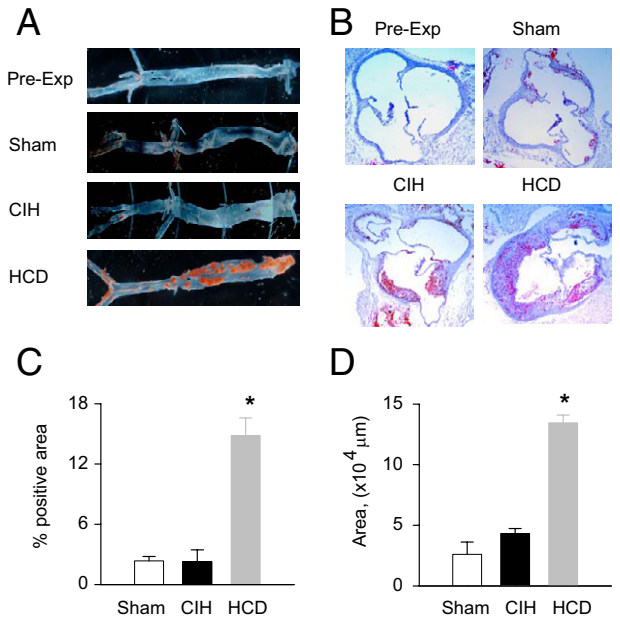

Figure 1. CIH exposure causes atherosclerosis in ApoE-KO mice. ApoE-KO mice were fed a normal chow diet and exposed to sham or CIH. A positive control group of ApoE-KO mice were fed a high cholesterol diet (HCD) but were not exposed to CIH. After 9 weeks of exposure, the *en face* aortic preparations and cross sections of aortic root were prepared and stained with Sudan IV or oil red O, respectively. **A** and **B:** Representative photographs of *en face* aortic preparations and cross sections of aortic root showing that Sudan IV- or oil red O-positive atherosclerotic lesions on aorta from mice exposed to CIH and HCD. No preexisting atherosclerotic lesions were detectable in both aortic preparations before CIH or HCD exposure (**A** and **B**, Pre-Exp). CIH exposure caused atherosclerotic lesions on cross sections of aortic root (**B**, Sham versus CIH) but not on *en face* aortic preparations (**A**, Sham versus CIH). HCD is a much stronger inducer of atherosclerosis (**A** and **B**, CIH versus HCD). Original magnification: ×4 (**A** and **B**). **C** and **D:** Atherosclerotic lesion areas on *en face* aortic preparations and cross sections of aortic root were quantified and expressed as a percentage of total aortic area (**C**) or as $\times 10^4$ μm (**D**). Means ± SEMs of eight animals (four males, four females) per group. $^*P < 0.05$, compared with the other two groups (analysis of variance followed by the Holm-Sidak method).

tended to be bigger in CIH-exposed mice than in sham-exposed mice (Figure 1). Thirty weeks of CIH exposure significantly increased atherosclerotic lesion areas on both aortic preparations (Figure 2). These results indicated that CIH exposure caused atherosclerotic lesions in an exposure time-dependent manner in ApoE-KO mice.

Atherosclerosis Induction Is Weaker when Exposed to CIH

We compared CIH- and HCD-induced atherosclerosis. After 9 weeks of exposure, HCD markedly increased atherosclerotic lesion areas on both *en face* aortic preparations and cross sections of aortic root (Figure 1, A and B), whereas CIH caused no detectable atherosclerotic lesions on the *en face* aortic preparations and a slightly increased lesion area on the cross sections of aortic root (Figure 1). Atherosclerotic lesion area on cross sections of aortic root was 3.1-fold larger in mice exposed to HCD than in mice exposed to CIH (Figure 1, C and 1D). Thus, CIH was a much weaker inducer of atherosclerosis, compared with HCD.

p50 Gene Deletion Augments CIH-Induced Atherosclerosis

To define the role of NF-κB in CIH-induced atherosclerosis, ApoE-p50-DKO mice were created, fed a ND, and exposed to sham and CIH. No atherosclerotic lesion was detectable on *en face* aortic preparations or cross sections of aortic root from ApoE-p50-DKO mice at the beginning of CIH exposure (data not shown). Compared with ApoE-KO mice, CIH exposure caused more pronounced atherosclerotic lesions in ApoE-p50-DKO mice (Figure 3, A and B). After 9 weeks of CIH exposure, atherosclerotic lesion areas on the *en face* aortic preparations and cross sections of aortic root of ApoE-p50-DKO mice were approximately 2.5-fold larger than that of ApoE-KO mice (Figure 3, C and D). Interestingly, atherosclerotic lesion area on cross section of aortic root was similar between ApoE-p50-DKO mice exposed to CIH for 9 weeks and ApoE-KO mice exposed to CIH for 30 weeks (Figures 2D versus 3D). Thus, ApoE-p50-DKO mice were more sensitive to CIH-induced atherogenesis, and blockade of p50 function augmented CIH-induced atherosclerosis.

Characterization of CIH Activated NF-κB Pathway in ApoE-KO Mice

To explain why p50 gene deletion augmented CIH-induced atherosclerosis, we first wanted to characterize CIH-activated NF-κB pathway and CIH-induced NF-κB complex in ApoE-KO mice. Our preliminary study showed that time course profiles of CIH-induced NF-κB activation and subunit composition of CIH-induced NF-κB complexes were

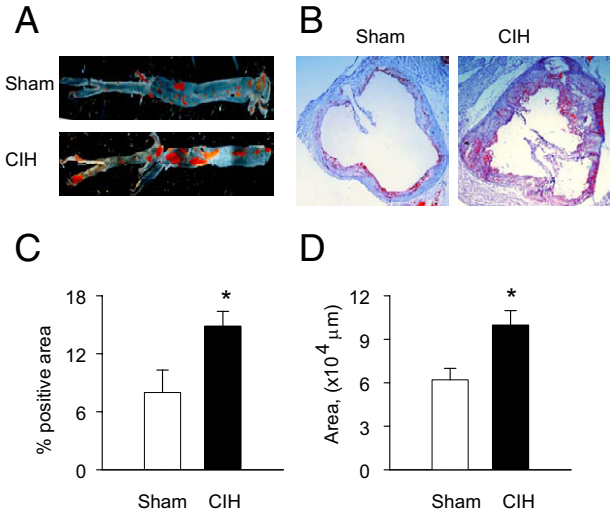

Figure 2. CIH exposure causes atherosclerosis in ApoE-KO mice. ApoE-KO mice were fed a normal chow diet and exposed to sham or CIH for 30 weeks. The *en face* aortic preparations and cross sections of aortic root were prepared and stained with Sudan IV or oil red O, respectively. **A** and **B:** Representative photographs of *en face* aortic preparations and cross sections of aortic root showing that Sudan IV- or oil red O-stained atherosclerotic lesions on the aorta from mice exposed for 30 weeks. Original magnification: ×4 (**A** and **B**). **C** and **D:** Atherosclerotic lesion areas on *en face* aortic preparations and cross sections of aortic root were quantified and expressed as a percentage of total aortic area (**C**) or as $\times 10^4$ μm (**D**). Means ± SEMs of five animals (all males) per group. $^*P < 0.05$, compared with sham-exposed group (unpaired *t* test).

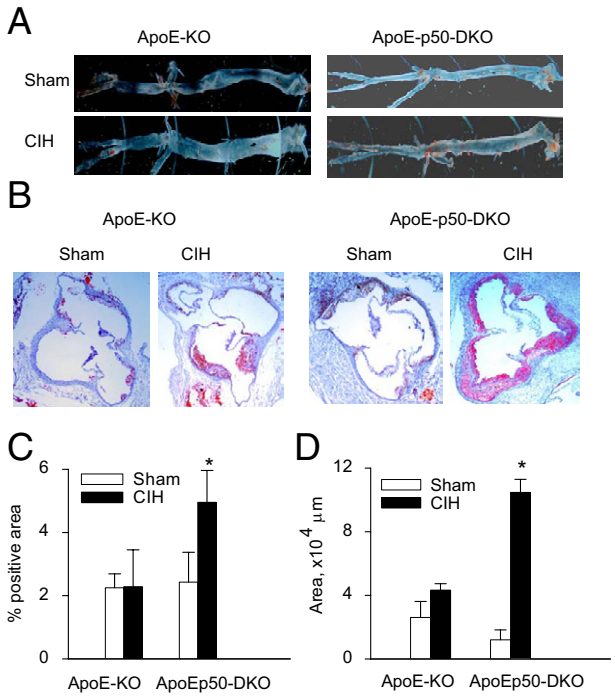

Figure 3. CIH-induced atherosclerosis is augmented in ApoE-p50-DKO mice. ApoE-KO and ApoE-p50-DKO mice were fed a normal chow diet and exposed to sham or CIH. After 9 weeks of exposure, the *en face* aortic preparations and cross sections of aortic root were stained with Sudan IV or oil red O, respectively. **A** and **B:** Representative photographs of *en face* aortic preparations and cross sections of aortic root showing that blockade of p50 function in ApoE-p50-DKO mice augments CIH-induced atherosclerosis. Original magnification: ×4 (**A** and **B**). **C** and **D:** Atherosclerotic lesion areas on *en face* aortic preparations and cross sections of aortic root were quantified and expressed as a percentage of total aortic area (**C**) or as $\times 10^4$ μm (**D**). Means ± SEMs of eight animals (four males, four females) per group. $^*P <$ 0.05, compared with the ApoE-KO-CIH group (Mann-Whitney rank sum test).

similar between aorta and liver (data not shown). We performed all characterization studies with the use of hepatic proteins to save aortas for more important analyses, such as atherosclerotic lesion analyses. Western blot analysis found that CIH had no effects on hepatic levels of TRAF3 and p100 proteins (Figure 4A), two key signaling molecules in the noncanonical NF-κB activation pathway,[35,36] but reduced hepatic level of I-κBα protein (Figure 4A),key signaling molecule of the canonical NF-κB activation pathway.[35,36]

Supershift assay showed that the CIH-induced NF-κB complex was significantly shifted by p50 or p50+p65, slightly shifted by C-Rel, but not shifted by p52 and Rel B antibodies (Figure 4B). P50+p65 antibodies caused a stronger supershifted band than p50 antibody alone. Thus, in ApoE-KO mice, CIH activated NF-κB via the canonical pathway. The CIH-induced NF-κB complex was composed predominantly of p50/p50 homodimer but also contained C-Rel/p50 and likely p65/p50 heterodimers (Figure 4B). P50 gene deletion inhibited CIH-induced NF-κB activity (Figure 4C).

p50 Gene Deletion Enhances CIH-Induced Inflammatory Response

We examined whether p50 gene deletion promoted atherosclerosis by enhancing the expression of proinflammatory genes, TNF-α, IL6, and iNOS. We chose to study these gene products because of their established roles in atherogenesis.[37–39] CIH exposure increased serum levels of TNF-α and IL-6 in ApoE-KO mice and further increased serum levels of the 2 cytokines in ApoE-p50-DKO mice (Figure 5, A and B).

IHC staining showed that CIH increased aortic iNOS and TNF-α expression in ApoE-KO mice and further increased iNOS and TNF-α expression in ApoE-p50-DKO mice (Figure 6, A, B, D, and E). Likewise, CIH caused an increase in ApoE-KO mice and a greater increase in ApoE-p50-DKO mice in aortic infiltration of Mac3-positive macrophages (Figure 6C). These results indicated that p50 gene deletion promoted inflammatory phenotype by enhancing NF-κB-regulated inflammatory gene expression.

p50 Gene Deletion Increases Serum Level of Cholesterol

Dyslipidemia is a major mechanism of atherogenesis[40]; we examined whether p50 gene deletion promoted development of dyslipidemia. Serum levels of lipids and lipoproteins in the four groups of mice were shown in Figure 7. CIH exposure did not significantly increase serum cholesterol level in ApoE-KO mice but significantly increased serum cholesterol level in ApoE-p50-DKO mice (Figure 7A). CIH had no significant effects on serum levels of triglycerides, HDL-cholesterol, and LDL-choles-

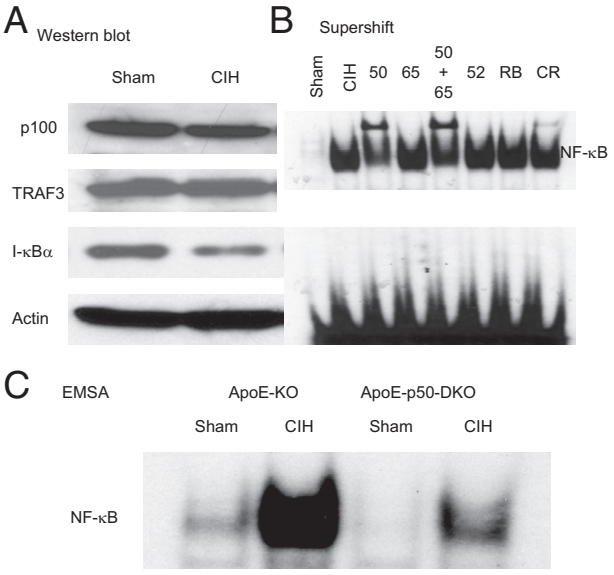

Figure 4. Characterization of CIH-activated NF-κB pathway. ApoE-KO and ApoE-p50-DKO mice were fed a normal chow diet and exposed to sham or CIH for 14 days. Hepatic levels of tumor necrosis factor (TNF) receptor associate factor 3 (TRAF3), p100/NF-κB2, I-κBα, and actin proteins and NF-κB activity were determined. **A:** Western blot photographs show cytoplasmic levels of TRAF3, p100, I-κBα, and actin proteins. CIH did not cause TRAF3 and p100 degradation, but it significantly reduced cytoplasmic level of I-κBα, indicating that CIH activates NF-κB via the canonical pathway in ApoE-KO mice. **B:** Supershift assay showing subunit composition of CIH-induced NF-κB complex in ApoE-KO mice. The CIH-induced NF-κB band was significantly shifted by p50 (50) or p50+p65 (50 + 65), slightly shifted by C-Rel (CR) but not shifted by p52 (52) or Rel B (RB) antibody. P50+p65 antibodies resulted in a stronger supershifted band than p50 antibody alone. **C:** Electrophoretic mobility shift assay (EMSA) autoradiograph showing that the CIH-induced NF-κB activity was greatly reduced in ApoE-p50-DKO mice.

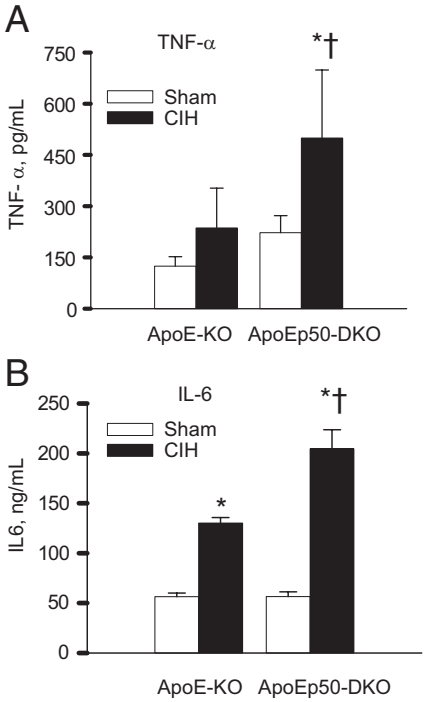

Figure 5. CIH-induced inflammatory mediator production is enhanced in ApoE-p50-DKO mice. ApoE-KO and ApoE-p50-DKO mice were fed a normal chow diet and exposed to sham or CIH for 9 weeks. Serum levels of tumor necrosis factor-α (TNF-α; **A**) and IL-6 (**B**) were determined by ELISA. CIH exposure resulted in significantly higher serum levels of TNF-α and IL-6 in ApoE-p50-DKO than in ApoE-KO mice. Means ± SEMs of six mice in each group. $^{*}P < 0.05$, compared with respective sham group; $^{\dagger}P < 0.05$, compared with ApoE-KO-CIH group (Kruskal-Wallis rank test followed by Student-Newman–Keuls method).

terol in either ApoE-KO or ApoE-p50-DKO mice (Figure 7, B–D). Thus, CIH exposure caused an elevated serum cholesterol level in ApoE-p50-DKO mice.

CIH Exposure Down-Regulates LDL Receptor Expression in ApoE-p50-DKO Mice

To explain why CIH exposure induced hypercholesterolemia in ApoE-p50-DKO mice, we compared the effects of CIH on hepatic expression of several key genes that regulate cholesterol biosynthesis, uptake, clearance, and reverse transport, HMG-CoA reductase, LDL receptor, ABCA1, SR-B1, and SREBF-2, between ApoE-KO and ApoE-p50-DKO mice. CIH exposure significantly down-regulated hepatic LDL receptor and HMG-CoA reductase expressions in ApoE-p50-DKO mice but not in ApoE-KO mice (Figure 8, A and B). CIH exposure did not significantly alter hepatic ABCA1 (Figure 8C), SR-B1 (Figure 8D) and SREBF-2 (Figure 8E) expressions in either ApoE-KO or ApoE-p50-DKO mice. These results suggested that CIH exposure may cause high serum cholesterol level in ApoE-p50-DKO mice by down-regulating LDL receptor expression.

Discussion

Atherosclerosis is a complex inflammatory disease of large arteries. To elucidate the mechanisms and pathways that link OSA-associated CIH and atherosclerosis, an animal model is of vital importance. Two mouse models of CIH-induced atherosclerosis have been reported.[10,14] Although studies that use these models have gained valuable information, both models have limitations. The CIH+HCD model cannot tell which response is evoked by CIH, which response is evoked by HCD, and which response is evoked by both.[10] In addition, HCD is several times more potent than CIH in inducing atherosclerosis. The stronger effect of HCD may overwhelm the weaker effect of CIH, particularly when ApoE-KO mice were used, which makes the assessment of independent effect of CIH very difficult. The second model is useful for studying CIH effect on disease progression,[14] but it cannot reveal CIH-induced early molecular and cellular

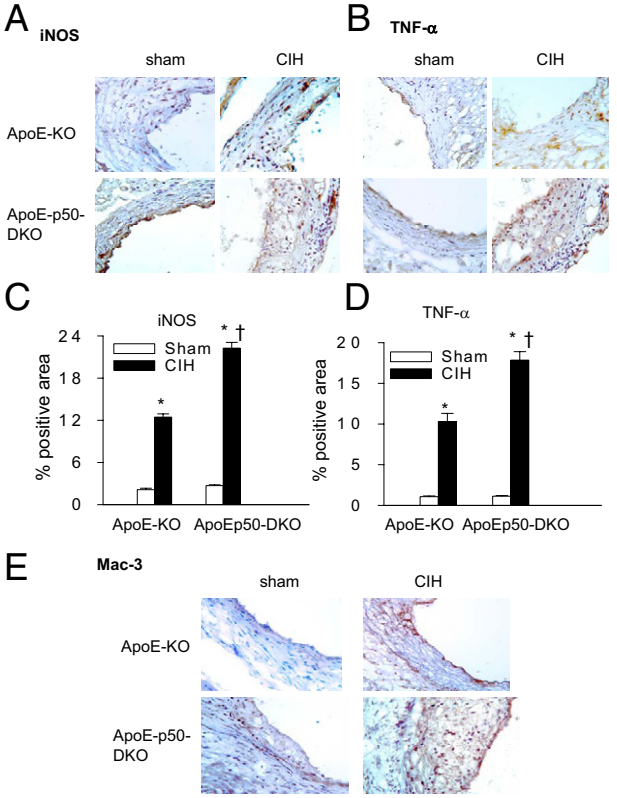

Figure 6. CIH-induced aortic inducible nitric oxide synthase (iNOS) and tumor necrosis factor-α (TNF-α) expression and macrophage infiltration are augmented in ApoE-p50-DKO mice. **A** and **B:** ApoE-KO and ApoE-p50-DKO mice were fed a normal chow diet and exposed to sham or CIH for 9 weeks. Aortic iNOS and TNF-α protein expression was detected by immunohistochemistry (IHC) staining with the use of specific antibodies for iNOS and TNF-α. **A:** IHC staining showed that CIH-induced aortic iNOS expression (dark brown dots) was augmented in ApoE-p50-DKO mice. **B:** IHC staining showed that CIH-induced aortic TNF-α expression (dark brown dots) was augmented in ApoE-p50-DKO mice. **C:** Quantitative analysis of the iNOS-positive area expressed as the percentage of total analyzed area. Means ± SEMs of five mice in each group. $^{*}P < 0.05$, compared with respective sham group; $^{\dagger}P < 0.05$, compared with ApoE-KO-CIH group (analysis of variance followed by Holm-Sidak method). **D:** Quantitative analysis of the TNF-α-positive area expressed as the percentage of total analyzed area. Means ± SEM of five mice in each group. $^{*}P < 0.05$, compared with respective sham group; $^{\dagger}P < 0.05$, compared with ApoE-KO-CIH group (Kruskal-Wallis rank test followed by Student-Newman–Keuls method). **E:** IHC staining showed CIH-induced aortic infiltration of Mac3-positive macrophages (dark brown dots) was augmented in ApoE-p50-DKO mice. Mice were fed a normal chow diet and exposed to sham or CIH for 9 weeks. Aortic macrophage infiltration was detected by IHC staining with the use of Mac3-specific antibodies. Original magnification, ×40 (A, B, and E).

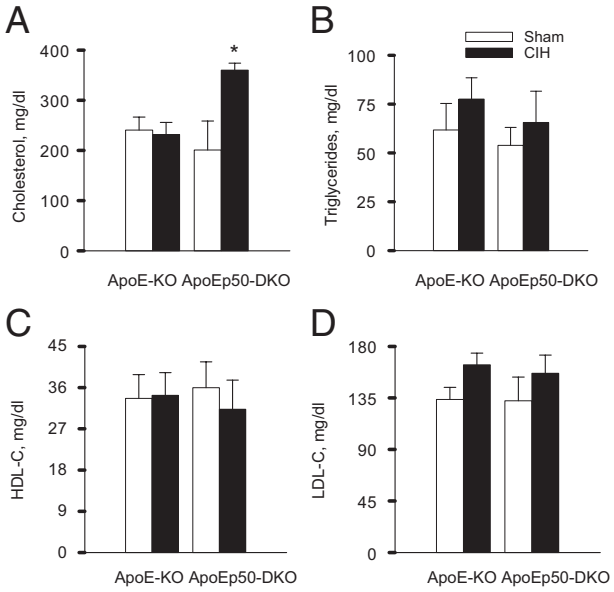

Figure 7. CIH causes hypercholesterolemia in ApoE-p50-DKO mice. ApoE-KO and ApoE-p50-DKO mice were fed a normal chow diet and exposed to sham or CIH for 9 weeks. Serum levels of cholesterol (**A**), triglycerides (**B**), high-density lipoprotein cholesterol (HDL-C; **C**), and low- density lipoprotein cholesterol (LDL-C; **D**) were measured with assay kits. CIH caused hypercholesterolemia in ApoE-p50-DKO but not in ApoE-KO mice. Means ± SEMs of six to eight mice in each group. $^*P < 0.05$, compared with ApoE-KO-CIH group (analysis of variance followed by the Holm-Sidak method).

events that lead to the initial formation and development of atherosclerotic lesions. Such information is crucial for understanding the mechanisms and pathways of CIH-induced atherosclerosis.

Recognizing the limitations, we herein tested two new models. We fed ApoE-KO and ApoE-p50-DKO mice a ND and exposed them to CIH at the age before spontaneous atherosclerotic lesions occurred. We demonstrated that CIH exposure caused atherosclerotic lesions in an exposure time-dependent manner in ApoE-KO mice that were fed a ND and had no preexisting atherosclerotic condition. ApoE-p50-DKO mice on a ND without preexisting atherosclerotic condition developed more pronounced atherosclerotic lesions after 9 weeks of CIH exposure. Thus, we have demonstrated two new mouse models of CIH-induced atherosclerosis.

Our models have advantages over the previously reported models[10,14] in that they avoid the confounder of HCD and allow studying CIH-triggered early molecular and cellular events that lead to the occurrence and development of atherosclerosis. Epidemiologic studies have found an independent association between OSA and atherosclerotic cardiovascular disease.[1–7] Atherosclerosis occurs in patients with OSA free of any other significant risk factor.[6] Compared with previously reported models, our models are more consistent with the notion that OSA is an independent risk factor for atherosclerosis.

The ApoE-p50-DKO mouse model may be particularly useful for studying CIH-induced atherosclerosis. ApoE-p50-DKO mice are significantly more sensitive than ApoE-KO mice to CIH-evoked atherogenesis. ApoE-p50-DKO and ApoE-KO mice exposed to CIH for 9 or 30 weeks, respectively, exhibited similar atherosclerotic lesion areas, whereas ApoE-p50-DKO mice exposed to CIH for 9 weeks had a significantly smaller area in spontaneously occurred atherosclerotic lesions than ApoE-KO mice exposed to CIH for 30 weeks.

A potential limitation for our models is the higher than normal serum level of cholesterol and altered serum lipoprotein profile in ApoE-KO mice.[22,23,41] Serum lipid and lipoprotein profiles in ApoE-p50-DKO mice have not been extensively characterized, but they appear to be similar to that of ApoE-KO mice. Fortunately, these mice have been continuously exposed to the dyslipidemia for a long time (since birth) before exposure to CIH.[41] Most of the changes caused by dyslipidemia have occurred before CIH exposure. The preexposure can significantly reduce the effect of dyslipidemia on CIH-evoked response. Study has shown that preexposure to dyslipidemia blunts subsequent responses to CIH,[17] likely through mechanisms of desensitization. This implies that the CIH-induced changes actually observed would be more cred-

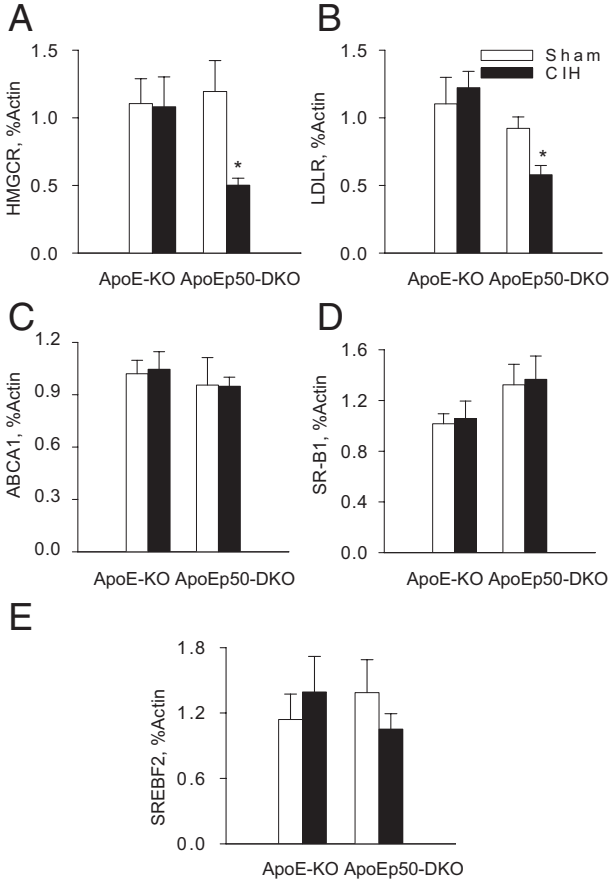

Figure 8. CIH exposure down-regulates hepatic low-density lipoprotein (LDL) receptor and HMG-CoA reductase (HMGCR) expression in ApoE-p50-DKO mice. ApoE-KO and ApoE-p50-DKO mice were fed a normal chow diet and exposed to sham or CIH for 9 weeks. Hepatic levels of mRNAs expressions of HMGCR (**A**), low-density lipoprotein receptor (LDLR; **B**), ATP-binding cassette transporter A1 (ABCA1; **C**), scavenger receptor class B1 (SR-B1; **D**), and sterol regulatory element-binding factor-2 (SREBF-2; **E**) were quantified with quantitative RT-PCR and normalized to level of β-actin mRNA. Means ± SEMs of seven mice per group. $^*P < 0.05$ compared with the other three groups (analysis of variance followed by Holm-Sidak method).

ible and the study conclusion more conservative. In the CIH+HCD model,[10] however, mice were exposed to HCD (and its resultant dyslipidemia) and CIH simultaneously. HCD- and CIH-evoked responses interfere with each other. More importantly, the much stronger effects of HCD may overwhelm the weaker effects of CIH, masking CIH effects.

An augmentation of CIH-induced atherosclerosis in ApoE-p50-DKO mice supports the notion that NF-κB p50 plays a protective role against CIH-induced atherosclerosis. One likely mechanism underlying the protection is the anti-inflammatory action of p50/p50 dimer. Compared with ApoE-KO mice, ApoE-p50-DKO mice had higher serum levels of TNF-α and IL-6, increased aortic iNOS and TNF-α expressions, and an increased aortic infiltration of Mac-3-positive macrophages, indicating that p50 gene deletion augmented CIH-induced systemic and vascular inflammation. Because of the established roles of these inflammatory mediators[37–39] and vascular inflammation in atherogenesis, these results suggest that NF-κB p50 protects against CIH-induced atherosclerosis by inhibiting CIH-induced inflammation.

Depending on models, context, stimuli, and partner protein with which p50 interacts, NF-κB p50 has both proinflammatory and anti-inflammatory effects.[42–47] P50 forms p50/p50/Bcl-3 (B-cell lymphoma 3-encoded protein) or p50/p50/HDAC-1 (histone deacetylase-1) repressor complex, which suppresses the transcriptional expression of inflammatory genes.[42,48] We demonstrated here that p50 plays an anti-inflammatory role in CIH-evoked inflammatory and atherogenic responses in ApoE-KO mice. Our result is consistent with the concept that NF-κB p50 is a repressor of inflammatory responses.[42–45] This result, however, does not necessarily conflict with our original hypothesis that NF-κB activation mediates CIH-induced atherosclerosis. Our demonstration that CIH caused a significantly reduced tissue level of I-κBα, but not TRAF3 or p100, indicates that CIH activates NF-κB via the canonical or typical pathway.[35,36,49] Supershift assay indicated that CIH-induced NF-κB complex contains three NF-κB subunits, with p50 being the predominant one. It is possible that in the presence of p50 (ApoE-KO mice) p50/c-Rel and/or possible p50/p65 heterodimers mediate the transactivation, and p50/p50 homodimer mediates the transrepression of CIH-stimulated NF-κB target genes. However, transactivation is able to override transrepression, resulting in increased expression of NF-κB target genes and atherosclerosis after CIH exposure. In the absence of p50 (ApoE-p50-DKO mice), p50/p50-mediated transrepression is eliminated and c-Rel and/or possible p65 mediated transactivation is enhanced, although through the formation of different NF-κB dimers, resulting in an augmented transcription of CIH-induced NF-κB target genes and atherosclerosis. In supporting this possibility, it was reported that c-Rel gene knockout significantly inhibited or blocked TNF-α, IL-6, and iNOS expression in macrophages stimulated with LPS+interferon-γ.[50] The transactivation function of p65 is well documented.[35] P50-KO mice are reported to have an enhanced p65-mediated transcription of inflammatory genes by a mechanism of p65 posttranslational modification.[44]

CIH exposure significantly increased the serum level of total cholesterol in ApoE-p50-DKO mice but not in ApoE-KO mice. Because hypercholesterolemia is a major pathogenic factor of atherosclerosis,[40] this result implies that p50 gene deletion may augment CIH-induced atherosclerosis by exacerbating hypercholesterolemia. To elucidate the mechanisms underlying the exacerbation, we compared hepatic expression of HMG-CoA reductase, the rate-limiting enzyme in cholesterol biosynthesis, LDL receptor, key receptor mediating LDL-mediated cholesterol uptake and clearance, and ABCA1 and SR-B1, molecules mediating HDL-mediated cholesterol reverse transport. We also examined hepatic expression of SREBF-2, the master regulator of cholesterol synthesis. We found that CIH exposure significantly down-regulated hepatic HMG-CoA reductase expression and had no effect on SREBF-2 expression, suggesting that an increased cholesterol biosynthesis may not be a major factor accounting for the high serum cholesterol level in ApoE-p50-DKO mice, although we did not measure HMG-CoA reductase activity. No difference in hepatic ABCA1 and SR-B1 expressions was observed between ApoE-KO and ApoE-p50-DKO mice, suggesting that inhibition of the HDL-mediated cholesterol reverse transport mechanism may not be a major factor. However, additional studies that examined the activities of the two receptors are needed to clarify the contribution of this mechanism. In ApoE-p50-DKO mice, CIH exposure down-regulated hepatic LDL receptor expression, associated with an elevated serum level of cholesterol. In ApoE-KO mice, CIH did not down-regulate LDL receptor expression, associated with no change in serum cholesterol level. Because LDL receptor is responsible for controlling the homeostasis of cholesterol in the blood stream, down-regulation of LDL receptor expression could impair the LDL-mediated cholesterol uptake and clearance mechanism, leading to an elevated serum cholesterol level. LDL receptor down-regulation is not the only factor. When the number of hepatic LDL receptors is reduced, serum LDL-cholesterol molecules cannot be taken up. A reduced LDL receptor expression in the liver is expected to be associated with an elevated serum level of LDL-cholesterol. However, serum level of LDL-cholesterol in the ApoE-p50-DKO-CIH group was not higher than that in the ApoE-KO-CIH group of mice, despite a significant decrease in hepatic LDL receptor expression and a 1.79-fold increase in serum total cholesterol level in the ApoE-p50-DKO mice. This result suggests that CIH exposure may hamper LDL formation, leading to an elevated serum level of free cholesterol in ApoE-p50-DKO mice. Further studies are necessary to fully elucidate the mechanisms by which p50 gene deletion impairs LDL formation and LDL-mediated cholesterol uptake and clearance after CIH exposure.

In summary, we have demonstrated two new mouse models of CIH-induced atherosclerosis. Exposure of ApoE-KO mice fed a ND and with no preexisting atherosclerotic condition to CIH induced atherosclerotic lesions in an exposure time-dependent manner. ApoE-p50-DKO

mice on a ND without preexisting atherosclerotic condition developed more pronounced atherosclerotic lesions after 9 weeks of CIH exposure. We showed that NF-κB p50 is protective against CIH-induced atherosclerosis. P50 protects against CIH-induced atherosclerosis by inhibiting CIH-induced inflammation and hypercholesterolemia. Our models can be useful tools for studying mechanisms and pathways of CIH-induced atherosclerosis. Our data provide new mechanistic insights into the mechanisms of CIH-induced atherosclerosis.

Acknowledgment

We thank Dr. Edmund Miller for help on mouse pulse oximeter measurement.

References

1. Mooe T, Franklin KA, Holmstrom K, Rabben T, Wiklund U: Sleep-disordered breathing and coronary artery disease: long-term prognosis. Am J Respir Crit Care Med 2001, 164:1910–1913
2. Yaggi HK, Concato J, Kernan WN, Lichtman JH, Brass LM, Mohsenin V: Obstructive sleep apnea as a risk factor for stroke and death. N Engl J Med 2005, 353:2034–2041
3. Quan SF, Gersh BJ: Cardiovascular consequences of sleep-disordered breathing: past, present and future: report of a workshop from the National Center on Sleep Disorders Research and the National Heart, Lung, and Blood Institute. Circulation 2004, 109:951–957
4. Somers VK, White DP, Amin R, Abraham WT, Costa F, Culebras A, Daniels S, Floras JS, Hunt CE, Olson LJ, Pickering TG, Russell R, Woo M, Young T: Sleep apnea and cardiovascular disease: an American Heart Association/American College of Cardiology Foundation scientific statement from the American Heart Association. Circulation 2008, 118:1080–1111
5. Mokhlesi B, Gozal D: Update in sleep medicine 2010. Am J Respir Crit Care Med 2010, 181:545–549
6. Lévy P, Pépin JL, Arnaud C, Baguet JP, Dematteis M, Mach F: Obstructive sleep apnea and atherosclerosis. Prog Cardiovasc Dis 2009, 51:400–410
7. Bradley TD, Floras JS: Obstructive sleep apnea and its cardiovascular consequences. Lancet 2009, 373:82–93
8. Fletcher EC, Costarangos C, Miller T: The rate of fall of arterial oxyhemoglobin saturation in obstructive sleep apnea. Chest 1989, 96:717–722
9. Flemons, WW. Clinical practice: obstructive sleep apnea. N Engl J Med 2002, 347:498–504
10. Savransky V, Nanayakkara A, Li J, Bevans S, Smith PL, Rodriguez A, Polotsky VY: Chronic intermittent hypoxia induces atherosclerosis. Am J Respir Crit Care Med 2007, 175:1290–1297
11. Savransky V, Jun J, Li J, Nanayakkara A, Fonti S, Moser AB, Steele KE, Schweitzer MA, Patil SP, Bhanot S, Schwartz AR, Polotsky VY: Dyslipidemia and atherosclerosis induced by chronic intermittent hypoxia are attenuated by deficiency of stearoyl coenzyme A desaturase. Circ Res 2008, 103:1173–1180
12. Jun J, Reinke C, Bedja D, Berkowitz D, Bevans-Fonti S, Li J, Barouch LA, Gabrielson K, Polotsky VY: Effect of intermittent hypoxia on atherosclerosis in apolipoprotein E-deficient mice. Atherosclerosis 2010, 209:381–386
13. Li RC, Haribabu B, Mathis SP, Kim J, Gozal D: Leukotriene B4 receptor-1 mediates intermittent hypoxia-induced atherogenesis. Am J Respir Crit Care Med 2011, 184:124–131
14. Arnaud C, Poulain L, Lévy P, Dematteis M: Inflammation contributes to the atherogenic role of intermittent hypoxia in apolipoprotein-E knock out mice. Atherosclerosis 2011, 219:425–431
15. Fletcher EC. Invited review: physiological consequences of intermittent hypoxia: systemic blood pressure. J Appl Physiol 200, 90:1600–1605
16. de Frutos S, Duling L, AlÒ D, Berry T, Jackson-Weaver O, Walker M, Kanagy N, González Bosc L: NFATc3 is required for intermittent hypoxia-induced hypertension. Am J Physiol Heart Circ Physiol 2008, 294:H2382–H2390
17. Li J, Thorne LN, Punjabi NM, Sun CK, Schwartz AR, Smith PL, Marino RL, Rodriguez A, Hubbard WC, O'Donnell CP, Polotsky VY: Intermittent hypoxia induces hyperlipidemia in lean mice. Circ Res 2005, 97:698–706
18. Li J, Bosch-Marce M, Nanayakkara A, Savransky V, Fried SK, Semenza GL, Polotsky VY: Altered metabolic responses to intermittent hypoxia in mice with partial deficiency of hypoxia-inducible factor-1alpha. Physiol Genomics 2006, 25:450–457
19. Greenberg H, Ye X, Wilson D, Htoo AK, Henderson T, Liu SF: Chronic intermittent hypoxia activates nuclear factor-kappaB in cardiovascular tissues in vivo. Biochem Biophys Res Commun 2006, 343:591–596
20. Arnaud C, Beguin PC, Lantuejoul S, Pepin JL, Guillermet C, Pelli G, Burger F, Buatois V, Ribuot C, Baguet JP, Mach F, Levy P, Dematteis M: The inflammatory preatherosclerotic remodeling induced by intermittent hypoxia is attenuated by RANTES/CCL5 inhibition. Am J Respir Crit Care Med 2011, 184:724–731
21. Fang G, Song D, Liu G, Ye X, Liu SF: Chronic intermittent hypoxia facilitates high fat diet-induced atherosclerosis by an NF-κB-dependent mechanism. Am J Respir Crit Care Med 2010, 181:A6636
22. Daugherty A: Mouse models of atherosclerosis. Am J Med Sci 2002, 323:3–10
23. Maeda N: Development of apolipoprotein E-deficient mice. Arterioscler Thromb Vasc Biol 2011, 31:1957–1962
24. Htoo AK, Greenberg H, Tongia S, Chen G, Henderson T, Wilson D, Liu SF: Activation of nuclear factor kappaB in obstructive sleep apnea: a pathway leading to systemic inflammation. Sleep Breath 2006, 10:43–50
25. Ryan S, Taylor CT, McNicholas WT: Selective activation of inflammatory pathways by intermittent hypoxia in obstructive sleep apnea syndrome. Circulation 2005, 112:2660–2667
26. Dyugovskaya L, Polyakov A, Ginsberg D, Lavie P, Lavie L: Molecular pathways of spontaneous and TNF-{alpha}-mediated neutrophil apoptosis under intermittent hypoxia. Am J Respir Cell Mol Biol 2011, 45:154–162
27. Ryan S, Taylor CT, McNicholas WT: Systemic inflammation: a key factor in the pathogenesis of cardiovascular complications in obstructive sleep apnea syndrome? Thorax 2009, 64:631–636
28. de Winther MP, Kanters E, Kraal G, Hofker MH: Nuclear factor kappaB signaling in atherogenesis. Arterioscler Thromb Vasc Biol 2005, 25:904–914
29. Pamukcu B, Lip GY, Shantsila E: The nuclear factor–kappa B pathway in atherosclerosis: a potential therapeutic target for atherothrombotic vascular disease. Thromb Res 2011, 128:117–123
30. Yang H, Roberts LJ, Shi MJ, Zhou LC, Ballard BR, Richardson A, Guo ZM: Retardation of atherosclerosis by overexpression of catalase or both Cu/Zn- superoxide dismutase and catalase in mice lacking apolipoprotein E. Circ Res 2004, 95:1075–1081
31. van Vlijmen BJ, van den Maagdenberg AM, Gijbels MJ, van der Boom H, HogenEsch H, Frants RR, Hofker MH, Havekes LM: Diet-induced hyperlipoproteinemia and atherosclerosis in apolipoprotein E3-Leiden transgenic mice. J Clin Invest 1994, 93:1403–1410
32. Ye X, Ding D, Zhou Z, Chen G, Liu SF: Divergent roles of endothelial NF-κB in multiple organ injury and bacterial clearance in murine models of sepsis. J Exp Med 2008, 205:1303–1315
33. Ding J, Song D, Ye X, Liu SF. A pivotal role of endothelial-specific NF-κB signaling in the pathogenesis of septic shock and septic vascular dysfunction. J Immunol 2009, 183:4031–4038
34. Lee EJ, Woodske ME, Zou B, O'Donnell CP: Dynamic arterial blood gas analysis in conscious, unrestrained C57BL/6J mice during exposure to intermittent hypoxia. J Appl Physiol 2009, 107:290–294
35. Liu SF, Malik AB: NF-κB activation as a pathologic mechanism of septic shock and inflammation. Am J. Physiol Lung Cell Mol Physiol 2006, 290:L622–L645
36. Vallabhapurapu S, Matsuzawa A, Zhang W, Tseng PH, Keats JJ, Wang H, Vignali DA, Bergsagel PL, Karin M: Nonredundant and complementary functions of TRAF2 and TRAF3 in a ubiquitination cascade that activates NIK-dependent alternative NF-kappaB signaling. Nat Immunol 2008, 9:1364–1370
37. Brånén L, Hovgaard L, Nitulescu M, Bengtsson E, Nilsson J, Jovinge S: Inhibition of tumor necrosis factor-alpha reduces atherosclerosis in apolipoprotein E knockout mice. Arterioscler Thromb Vasc Biol 2004, 24:2137–2142

38. Huber SA, Sakkinen P, Conze D, Hardin N, Tracy R: Interleukin-6 exacerbates early atherosclerosis in mice. Arterioscler Thromb Vasc Biol 1999, 19:2364–2367
39. Kuhlencordt PJ, Chen J, Han F, Astern J, Huang PL: Genetic deficiency of inducible nitric oxide synthase reduces atherosclerosis and lowers plasma lipid peroxides in apolipoprotein E-knockout mice. Circulation 2001, 103:3099–3104
40. Steinberg D: Hypercholesterolemia and inflammation in atherogenesis: two sides of the same coin. Mol Nutr Food Res 2005, 49:995–998
41. Signori E, Rinaldi M, Fioretti D, Iurescia S, Seripa D, Perrone G, Norata GD, Catapano AL, Fazio VM: ApoE gene delivery inhibits severe hypercholesterolemia in newborn ApoE-KO mice. Biochem Biophys Res Commun 2007, 361:543–548
42. Elsharkawy AM, Oakley F, Lin F, Packham G, Mann DA, Mann J: The NF-kappaB p50: p50:HDAC-1 repressor complex orchestrates transcriptional inhibition of multiple pro-inflammatory genes. J Hepatol 2010, 53:519–527
43. Yang HT, Wang Y, Zhao X, Demissie E, Papoutsopoulou S, Mambole A, O'Garra A, Tomczak MF, Erdman SE, Fox JG, Ley SC, Horwitz BH: NF-κB1 inhibits TLR-induced IFN-β production in macrophages through TPL-2-dependent ERK activation. J Immunol 2011, 186: 1989–1996
44. Rajendrasozhan S, Chung S, Sundar IK, Yao H, Rahman I: Targeted disruption of NF-{kappa}B1 (p50) augments cigarette smoke-induced lung inflammation and emphysema in mice: a critical role of p50 in chromatin remodeling. Am J Physiol Lung Cell Mol Physiol 2010, 298:L197–L209
45. Cao S, Zhang X, Edwards JP, Mosser DM: NF-kappaB1 (p50) homodimers differentially regulate pro- and anti-inflammatory cytokines in macrophages. J Biol Chem 2006, 281:26041–26050
46. Wang D, Paz-Priel I, Friedman AD: NF-kappa B p50 regulates C/EBP alpha expression and inflammatory cytokine-induced neutrophil production. J Immunol 2009, 182:5757–5762
47. Fakhrzadeh L, Laskin JD, Laskin DL: Ozone-induced production of nitric oxide and TNF-alpha and tissue injury are dependent on NF-kappaB p50. Am J Physiol Lung Cell Mol Physiol 2004, 287:L279–L285
48. Grundström S, Anderson P, Scheipers P, Sundstedt A: Bcl-3 and NFkappaB p50-p50 homodimers act as transcriptional repressors in tolerant CD4+ T cells. J Biol Chem 2004, 279:8460–8468
49. Perkins ND: Integrating cell-signalling pathways with NF-kappaB and IKK function. Nat Rev Mol Cell Biol 2007, 8:49–62
50. Lamhamedi-Cherradi SE, Zheng S, Hilliard BA, Xu L, Sun J, Alsheadat S, Liou HC, Chen YH: Transcriptional regulation of type I diabetes by NF-kappa B. J Immunol 2003, 171:4886–4592